Proton-impact excitation of lithium using a time-dependent close-coupling method

Teck-Ghee Lee and M. S. Pindzola
Department of Physics, Auburn University, Auburn, Alabama 36849, USA
(Received 12 October 2011; published 15 November 2011)

A time-dependent close-coupling method, formulated within the framework of a rotational function expansion in two-dimensional cylindrical coordinates, is used to investigate excitation processes in proton-lithium collisions. As a first check, the calculated Li($1s^2 2s$) → Li($1s^2 2p$) excitation cross sections are compared and shown to be in reasonable agreement with the previous Cartesian lattice time-dependent Schrödinger equation results for collision energies at 5, 10, and 15 keV. As a result, additional calculations are carried out to determine the cross sections not only for the Li($1s^2 2s$) → Li($1s^2 2p$) transitions, but also for the Li($1s^2 3l$) transitions for a wider range of proton-impact energies from 2 to 50 keV. Reasonable agreement is found when further comparison of the dominant Li($1s^2 2p$) excitation cross sections is made with data obtained from crossed-beams experiments and other close-coupling methods. With the present extensive and large-scale calculations, the convergence for the reported results is also addressed, especially for the less-dominant Li($1s^2 3l$) transitions, with respect to the box sizes, number of coupled channels, and propagation time.

DOI: 10.1103/PhysRevA.84.052712 PACS number(s): 34.50.Fa, 34.70.+e

I. INTRODUCTION

Excitation processes of atomic lithium, the simplest quasi-one-electron atom, due to proton-impact is not only of fundamental interest, but also of practical importance for diagnostics of magnetically confined fusion plasmas by means of lithium beam spectroscopy [1,2]. Analysis of the emission lines of the injected lithium atoms at the edge of a tokamak plasma enables one to extract valuable information, such as radial electron density, concentrations and temperatures of impurity ions in the plasma. Reliable diagnostics therefore require accurate determination not only of electron-transfer cross sections, but also of excitation cross sections.

Experimental measurements of excitation cross sections based on a crossed-beams technique for a lithium target were carried out a number of years ago by Aumayr *et al.* [3–5]. On the theoretical side, there has been quite a number of predictions [6–11], since quasi-one-electron lithium is a good candidate for testing theoretical treatments of one-electron processes in few-electron atomic systems. Among the several theoretical methods used to treat the excitation processes in ion-atom collisions, the most elaborate and accurate methodologies are the atomic (or molecular) orbitals basis-set expansion methods [7,8,11] and the direct numerical solution of the time-dependent Schrödinger equation (TDSE) on a multidimensional lattice [9]. The latter method discretizes the TDSE on either a uniform or nonuniform three-dimensional (3D) spatial mesh and the resultant lattice TDSE is readily solved using a parallel supercomputer.

Although the lattice TDSE method has proven successful in describing not only one-electron excitation but also capture and ionization processes found in a number of fundamental ion-atom collision systems (e.g., $p + \mathrm{H}$ [12,13], $p + \mathrm{Li}$ [9,14,15], and $\mathrm{Be}^{4+} + \mathrm{H}$ [16]), a significant amount of computation time is required. For a realistic ion-atom collision problem and for a given projectile incident energy, the typical computation time for a TDSE calculation (based on a semiclassical impact-parameter approximation) grows like $N^3 N_b$, where N is the number of grid points and N_b is the number of impact parameters. This $N^3 N_b$ factor is a main concern as it restricts the capability of the method, even with the available massively parallel supercomputers, for accurately treating larger ion-atom collision systems. For the same reason, the study of the energy-dependent inelastic cross sections has to be restricted to a handful of energy points. Furthermore, extending the method to higher dimensions will make the computation even longer. A better theoretical approach to the problem, but based on reduced dimensionality within the direct numerical solution of TDSE formalism, is therefore worthwhile and highly desired.

As a possible solution, a three-dimensional TDSE method was recently formulated within the framework of rotational function close-coupling expansion in two-dimensional (2D) cylindrical coordinates [17]. As a proof of principle and a check, the method was employed to calculate excitation cross sections from the ground state of the hydrogen atom to the $2l$ and $3l$ excited states for $p + \mathrm{H}$ collisions at a proton-incident energy of 40 keV. The results were found to be in good agreement with the 3D Cartesian lattice time-dependent Schrödinger equation (LTDSE) as well as other competitive theoretical calculations. Here, we extend the 2D cylindrical time-dependent close-coupling (TDCC) method to investigate the direct excitation of Li($1s^2 2s$) due to 2 to 50 keV proton impact.

In previous work [9], the 3D Cartesian LTDSE method has been used to calculate the cross sections for Li($1s^2 2s$) → Li($1s^2 2p$) and Li($1s^2 2s$) → Li($1s^2 3l$) states at three proton-impact energies of 5, 10, and 15 keV. Although the results for the dominant Li($1s^2 2s$) → Li($1s^2 2p$) excitation were found to be in accord with the experimental data of Aumayr *et al.* [3–5], the accuracy of the cross sections, particularly for the weaker Li($1s^2 3l$) transitions, still remains uncertain due to the above reasons. As a result, a detailed study is carried out herein with emphasis on (i) the development of a local exchange potential in cylindrical coordinates to describe a quasi-one-electron atom such as lithium; (ii) checking whether, by incorporating such a potential into the recently developed cylindrical time-dependent close-coupling (TDCC) method, one could reasonably reproduce the previous results from the LTDSE calculations and other benchmarked theoretical

data; (iii) a convergence study for the present excitation cross sections with respect to different box sizes, number of coupled channels, and propagation time; and (iv) a proper energy-dependent study of the excitation cross sections; that is, at least a decade of energy points.

The rest of the article is organized as follows: a review of the time-dependent close-coupling method in the cylindrical representation is presented in Sec. II, the results for excitation cross sections from the ground state of atomic Li to the $1s^2 2p$ and $1s^2 3l$ configurations are presented and discussed in Sec. III, and a brief summary is given in Sec. IV. Atomic units (a.u.) are used throughout unless otherwise indicated.

II. THEORETICAL METHOD

We shall briefly recapitulate the essence of the time-dependent close-coupling method in cylindrical coordinates [17]. For a bare-ion projectile with a nuclear charge of Z_p colliding with a one-active-electron atomic target with a nuclear charge of Z_t, we solve the time-dependent Schrödinger equation given by

$$i\frac{\partial \Psi(\vec{r}_e,t)}{\partial t} = \left\{-\frac{1}{2}\nabla^2 - \frac{Z_t}{|\vec{r}_e|} + V_{HX}(r_e) - \frac{Z_p}{|\vec{r}_e - \vec{r}_p(t)|}\right\} \times \Psi(\vec{r}_e,t), \quad (1)$$

where $V_{HX}(r_e)$ is the Hartree-Slater local exchange potential and $\vec{r}_e$ and $\vec{r}_p$ denote the target electron position vector and the projectile ion position vector, respectively.

The total electronic wave function can be expressed in cylindrical coordinates and expanded in rotational functions:

$$\Psi(\vec{r}_e,t) = \sum_m \frac{P_m(\rho,z,t)}{\sqrt{\rho}}\Phi_m(\phi), \quad (2)$$

where $\Phi_m(\phi) = \frac{e^{im\phi}}{\sqrt{2\pi}}$. Substituting Eq. (2) into Eq. (1) results in time-dependent close-coupling equations in the cylindrical representation (TDCC ρz), given by

$$i\frac{\partial P_m(\rho,z,t)}{\partial t} = T_m(\rho,z)P_m(\rho,z,t) + \sum_{m'} V_{m,m'}(\rho,z,t)P_{m'}(\rho,z,t), \quad (3)$$

where

$$T_m(\rho,z) = K(\rho,z) + \frac{m^2}{2\rho^2} - \frac{Z_t}{\sqrt{\rho^2+z^2}} + V_{HX}(\rho,z), \quad (4)$$

$K(\rho,z)$ is the kinetic energy operator, $V_{HX}(\rho,z)$ is the Hartree-Slater local exchange potential in cylindrical coordinates, and

$$V_{m,m'}(\rho,z,t) = -Z_p \sum_\lambda \frac{(r_e,r_p)^\lambda_<}{(r_e,r_p)^{\lambda+1}_>} \sum_q \frac{(\lambda-|q|)!}{(\lambda+|q|)!} \times P_\lambda^{|q|}(\cos(\theta_e))P_\lambda^{|q|}(\cos(\theta_p)). \quad (5)$$

In this collision-energy regime, it is reasonable to assume a straight-line-trajectory approximation, such that $r_e = (\rho^2+z^2)^{1/2}$, $\cos(\theta_e) = z/r_e$, $r_p = [b^2+(z_0+vt)^2]^{1/2}$, and $\cos(\theta_p) = (z_0+vt)/r_p$, where $P_\lambda^{|q|}(\cos(\theta))$ is an associated Legendre function.

The TDCC equations are readily solved using lattice techniques to obtain a discrete representation of the wave functions $P_m(\rho,z,t)$ and all associated operators on a uniform ρz mesh. The lowest-order finite difference representation of the kinetic energy operator is given by

$$K_{i,j}P_{i,j}(t) = -\left\{\frac{[c_i^+ P_{i+1,j}(t) + c_i^- P_{i-1,j}(t) - 2P_{i,j}(t)]}{2(\Delta\rho)^2}\right\} - \left\{\frac{[P_{i,j+1}(t) + P_{i,j-1}(t) - 2P_{i,j}(t)]}{2(\Delta z)^2}\right\}, \quad (6)$$

with the coefficients $c_i^+ = (\rho_{i+1/2})/\sqrt{\rho_i\rho_{i+1}}$ and $c_i^- = (\rho_{i-1/2})/\sqrt{\rho_i\rho_{i-1}}$.

The initial condition for the solution of the TDCC equations is given by

$$P_m(\rho,z,t=0) = P_{2s0}(\rho,z)\Phi_0(\phi)\delta_{m,0}. \quad (7)$$

Transition probabilities for proton-impact excitation processes are found by time propagating the close-coupling equations based on an explicit algorithm given by

$$P(t+\Delta t) = -2i\Delta t H(t)P(t) + P(t-\Delta t), \quad (8)$$

where $H(t)$ is the full time-dependent Hamiltonian. Tracing the full time evolution of the wave functions, probabilities for state-selective excitation for a given projectile energy and impact parameter are obtained via

$$\mathcal{P}_{nlm}(E,b) = \left|\int d\vec{r}_e \Psi^*_{nlm}(\vec{r}_e)\,\Psi(\vec{r}_e,t\to\infty)\right|^2, \quad (9)$$

and hence their corresponding excitation cross sections are given by

$$\sigma_{nlm}(E) = 2\pi\int_0^\infty bdb\mathcal{P}_{nlm}(E,b). \quad (10)$$

Note that a masking function is implemented in order to eliminate the spurious reflection of the waves at the lattice boundary.

III. RESULTS

A. Comparison with previous work

We first checked the present cylindrical coordinates TDCC method against the previous Cartesian coordinates LTDSE method [9] for proton-impact excitation of Li. The radial Hartree-Slater local exchange potential is given by

$$V_{HX}(r_e) = 2\int dr'_e \frac{P^2_{1s}(r'_e)}{r_{e>}} - \alpha\left(\frac{24\rho(r_e)}{\pi}\right)^{\frac{1}{3}}, \quad (11)$$

where α is a freely adjustable parameter, $\rho(r) = 2P^2_{1s}(r_e)/(4\pi r_e^2)$ is the radial probability density, and $P_{1s}(r_e)$ is the bound radial orbital obtained from solving the Hartree-Fock equations [18] for $Li^+(1s^2)$. Following previous work [9], we diagonalize the radial Hamiltonian

$$H(r_e) = -\frac{1}{2}\frac{\partial^2}{\partial r_e^2} + \frac{l(l+1)}{2r^2} - \frac{Z_t}{r_e} + V_{HX}(r_e), \quad (12)$$

for $l=0$ and $Z_t=3$ on a 300-point radial mesh with $\Delta r_e = 0.2$. For $\alpha = 0.74$ the energy of the $2s$ state is in good agreement with the experimental value of -5.39 eV [19]. In order to prevent the $P_m(\rho,z,t)$ wave functions from collapsing into the $Li(1s^2)$ core during the time-propagation

of the close-coupling equations, we may replace $V_{HX}(\rho,z)$ with a pseudopotential $V_{PP}(\rho,z)$ constructed by eliminating the inner node of the $P_{2s}(r_e)$ orbital based on an established procedure [20]. Interpolation using $r_e = (x^2+y^2+z^2)^{1/2}$ and $r_e = (\rho^2+z^2)^{1/2}$ allows the construction of $V_{PP}(x,y,z)$ and $V_{PP}(\rho,z)$. In the Cartesian-coordinate LTDSE method, the ground and excited states were obtained by relaxation of the Hamiltonian in imaginary time since diagonalization of the Hamiltonian

$$H(x,y,z) = -\frac{1}{2}\left(\frac{\partial^2}{\partial x^2} + + \frac{\partial^2}{\partial y^2} + \frac{\partial^2}{\partial z^2}\right) - \frac{Z_t}{\sqrt{(x^2+y^2+z^2)}} + V_{PP}(x,y,z) \quad (13)$$

was not feasible. Upon relaxation, the energy of the $2s$ state was found to be in good agreement with the experimental value of -5.39 eV [19], but the $2p$ states were found to be at-3.12 eV, considerably higher than the the experimental value of -3.54 eV [19]. In the cylindrical-coordinate TDCC method the ground and excited states are obtained by diagonalization of the Hamiltonian

$$H_m(\rho,z) = K(\rho,z) + \frac{m^2}{2\rho^2} - \frac{Z_t}{\sqrt{\rho^2+z^2}} + V_{PP}(\rho,z). \quad (14)$$

For the same choice of $\alpha = 0.74$ the energy of the $2s$ state is in good agreement with the experimental value of -5.39 eV [19], but the $2p$ states were found to be at -3.13 eV, again considerably higher than the the experimental value of -3.54 eV [19]. See Table I for examples.

To further cross check the present method against the previous LTDSE results, we carried out the TDCC calculation using the equivalent LTDSE parameters given in Ref. [9] (e.g., a 160×320 mesh with $\Delta\rho = \Delta z = 0.2$ a.u. to form a cylinder of ρ: $0 \rightarrow +32$ and z: $-32 \rightarrow +32$, a set of 23 impact parameters ranging from 0 to 20 a.u., and the same starting and ending projectile-traveling journey). At 15 keV collision energy, we found with the present approach the Li($1s^2 2p$) cross section to be 37.0×10^{-16} cm^2 while the LTDSE gave a value of 34.9×10^{-16} cm^2. At the lower energy of 5 keV, the same state-selective excitation cross section turned out to be 25.0×10^{-16} cm^2 as opposed to the LTDSE value of 22.8×10^{-16} cm^2. This degree of agreement serves as a litmus test for the present TDCC calculation.

TABLE I. Lithium-atom binding energies (in eV) and energy gaps (in eV) between the ground and higher states.

nl	NIST [19]	$\alpha = 0.74$	$\alpha = 0.25$	$\alpha = 0.74$ [9]
$2s$	-5.392	-5.397	-5.416	-5.38
$2p_0$	-3.544	-3.130	-3.570	-3.12
$2p_{\pm1}$		-3.129	-3.560	
$3s$	-2.019	-2.015	-2.026	-2.01
$3p_0$	-1.558	-1.514	-1.563	-1.41
$3p_{\pm1}$		-1.513	-1.560	
$3d_0$	-1.513	-1.416	-1.515	-1.51
$3d_{\pm1}$		-1.416	-1.515	
$3d_{\pm2}$		-1.513	-1.514	
$\Delta E_{2s\text{-}2p}$	1.848	2.267	1.846	2.26
$\Delta E_{2s\text{-}3s}$	3.373	3.382	3.388	3.37
$\Delta E_{2s\text{-}3p}$	3.834	3.883	3.856	3.97
$\Delta E_{2s\text{-}3d}$	3.879	3.949	3.901	3.87

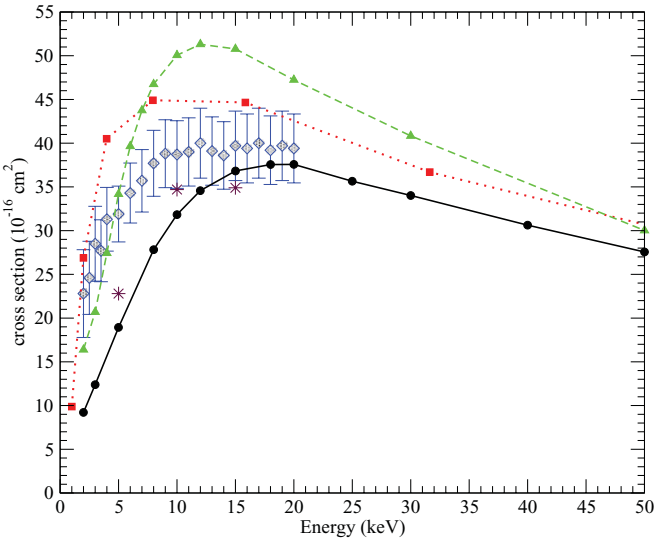

FIG. 1. (Color online) Proton-impact excitation cross sections for the Li($1s^2 2p$) as a function of collision energy. Black circles with solid line show present TDCC ($\alpha = 0.74$), green triangles with dashed line show present TDCC ($\alpha = 0.25$), purple stars show LTDSE [9], red squares with dotted line show B-spline AOCC method [11], and blue diamonds with error bars show experimental measurements [3–5].

With this level of confidence, we carried out additional and larger TDCC calculations by increasing the spatial extent to ρ: $0 \rightarrow +48$ a.u. by z: $-60 \rightarrow +60$ a.u. cylinder with uniform step sizes of $\Delta\rho = \Delta z = 0.2$, and by considering that the projectile travels for a longer distance; that is, from an initial position of $z_i = -30$ a.u. to a final position of $z_f = +240$ a.u. The scattering calculations were also carried out for 13 different collision energies ranging from 2.0 to 50.0 keV. The resulting excitation cross sections on an absolute scale for the Li($1s^2 2s$) $\rightarrow$ Li($1s^2 2p$) transition as function of collision energy are shown in Fig. 1. Comparing the present large-scale TDCC with the previous LTDSE results, the agreement again appears to be reasonable. This indicates that a scattering calculation carried out with a reasonable box size that could accommodate the L-shell electron cloud will yield reasonable excitation cross sections for Li($1s^2 2p$). But, as we will discuss next, this may not the case for transitions to the weaker M-shell.

B. Core-orthogonalization calculations

So far, we have shown that our TDCC and the LTDSE results are in reasonable agreement for the same choice of α. But with $\alpha = 0.74$, the excited-state energies are found to be less than satisfactory. Thus, improved excited-state energies are much desired. Without doing the imaginary-time Hamiltonian relaxation, we may obtain the ground and excited states by diagonalizing the Hamiltonian

$$H_m(\rho,z) = K(\rho,z) + \frac{m^2}{2\rho^2} - \frac{Z_t}{\sqrt{\rho^2+z^2}} + V_{HX}(\rho,z). \quad (15)$$

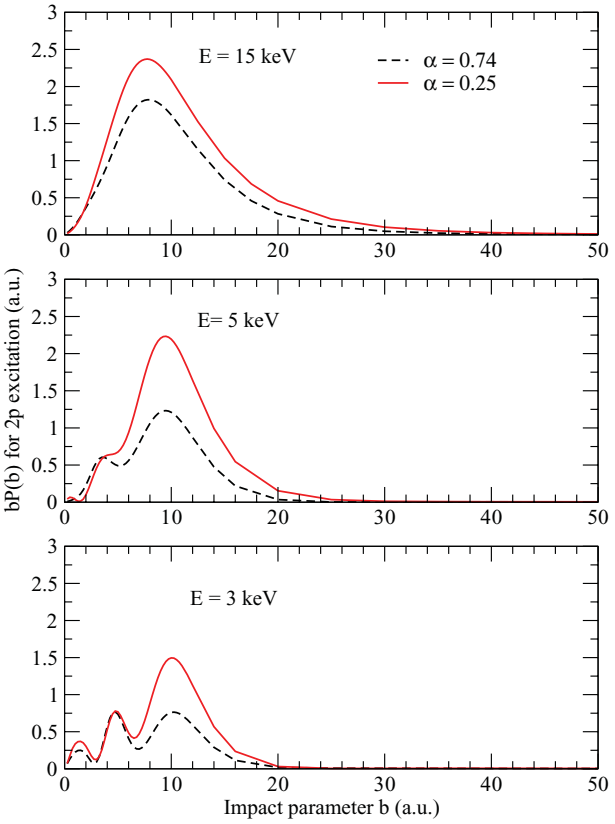

FIG. 2. (Color online) Impact-parameter-weighted Li($1s^2 2p$) excitation probability as a function of impact parameter b. Black dashed line shows present TDCC ($\alpha = 0.74$) and red solid line shows present TDCC ($\alpha = 0.25$).

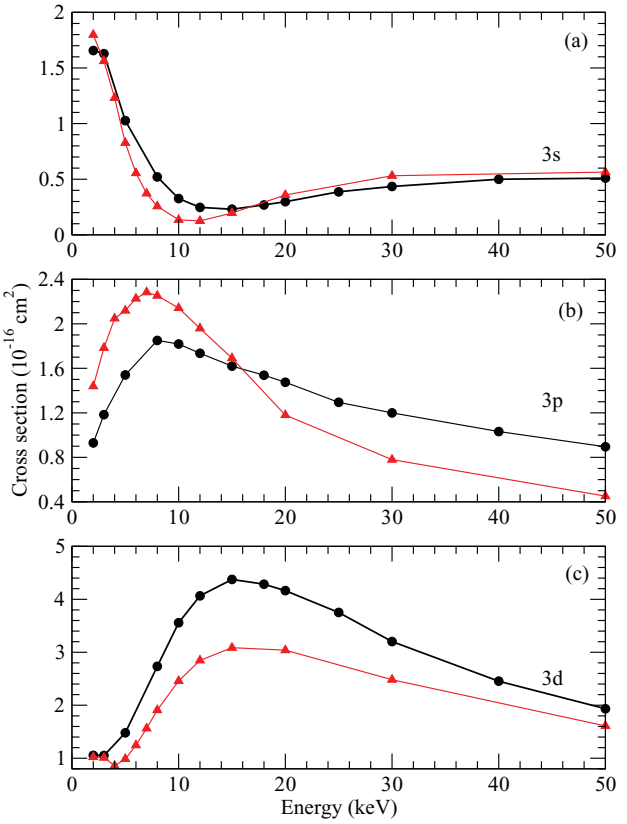

FIG. 3. (Color online) Proton-impact excitation cross sections for Li($1s^2 3s$), Li($1s^2 3p$), and Li($1s^2 3d$) as a function of collision energy. Black circles with solid line show present TDCC ($\alpha = 0.74$) and red triangles with solid line show present TDCC ($\alpha = 0.25$).

For the choice of $\alpha = 0.25$, shown in Table I, not only do we see that the energy of the $2s$ state remains in good agreement with the experimental value of -5.39 eV, but also all the excited states have been significantly improved and found to be in good agreement with the experimental values.

Similar TDCC calculations are then carried out with core-orthogonalization at each time step according to

$$\tilde{P}_m(\rho,z,t) = P_m(\rho,z,t) - P_{1s0}(\rho,z) \iint d\rho' dz' P_{1s0}(\rho',z') \times P_m(\rho',z',t) \quad (16)$$

in order to avoid the collapsing of the $P_m(\rho,z,t)$ wave functions into the Li($1s^2$) core. Figure 1 shows the present Li($1s^2 2p$) cross sections as a function of collision energy together with the results obtained from the previous $\alpha = 0.74$ calculation, a recent large-scale atomic orbitals close-coupling calculation based on a B-spline basis-set expansion method [11] and crossed-beams experiments [3–5]. Although the present results are larger compared to the $\alpha = 0.74$ calculation, both TDCC calculations are in reasonable agreement with the experimental data and atomic-orbital close-coupling (AOCC) calculations, The common feature of Li($1s^2 2p$) excitation cross sections as a function of energy is also reproduced by the theories.

We illustrate the impact-parameter-weighted Li($1s^2 2p$) excitation probability at collision energies of 3, 5, and 15 keV for two different values of α in Fig. 2. The probabilities calculated with $\alpha = 0.25$ are consistently larger compared with the $\alpha = 0.74$ values for all energies shown. Although their magnitudes are different, the probability distributions display a complementary trend. By examining the $\Delta E_{2s\text{-}2p}$ energy gap given in Table I, the disagreement in probability magnitude, and hence the cross sections, may be attributed to the difference in the $\Delta E_{2s\text{-}2p}$ energy found between the two calculations. The reason one sees a higher transition-probability yield is because the $\Delta E_{2s\text{-}2p}$ energy gap found for the $\alpha = 0.25$ calculation is indeed 42% smaller than the one with $\alpha = 0.74$. It is important to note that the α value is adjusted so that the Li atomic orbital energies agree as closely as possible with the experimental binding energies recommended by NIST.

Figure 3 displays the excitation cross sections for the less dominant Li($1s^2 2s$) $\rightarrow$ Li($1s^2 3s$), Li($1s^2 3p$), and Li($1s^2 3d$) transitions as a function of collision energy for the two α values. Only the Li($1s^2 3s$) configuration shows agreement between the two calculations. When comparing the LTDSE data (e.g., see Table III in Ref. [9]) with these values for proton-impact energies of 5, 10, and 15 keV, the LTDSE results turn out to be only qualitatively comparable to the TDCC calculations. This, as will be argued next, may be attributed to the inadequacy of the box size used in the earlier LTDSE calculations. As far as we know, there are no experimental data to compare with for the present Li($1s^2 3l$) excitation cross sections.

C. On convergence of the cross sections

We now discuss the convergence of our cross sections with respect to different box sizes and to the number of rotational functions. It is important to note that we restrict the following presentations to the calculations for the choice of $\alpha = 0.74$, since extensive calculations were performed using this value in order to check against the earlier LTDSE method [9] in the first place. Besides, except for the cross-section magnitude, the conclusions drawn from the convergence study of the cross section with respect to different box sizes, the number of coupled rotational channels, the propagation time, would not be any different from the calculations performed with the choice of $\alpha = 0.25$.

We present excitation probabilities for the $1s^2 2p$ and $1s^2 3l$ configurations as functions of impact parameter in Fig. 4 at the two incident energies of 5 and 15 keV. Calculations were carried out for three different box sizes: TDCC-A, TDCC-B, and TDCC-C with (ρ: $0 \rightarrow +48$, z: $-60 \rightarrow +60$), (ρ: $0 \rightarrow +40$ and z: $-43 \rightarrow +43$) and (ρ: $0 \rightarrow +32$ and z: $-32 \rightarrow +32$), respectively. First, notice that the resulting probabilities from both the TDCC-A and TDCC-B calculations are practically identical, indicating that the cross sections presented have converged with respect to the largest box. Second, in contrast to a hydrogen target, note that a larger impact parameter is required in order for some transition probabilities to achieve satisfactory convergence. Third, it is found that the general shape of the excitation probability changes dramatically from one collision energy to another. For example, comparing the first frame of Figs. 4(a) and 4(b), the Li($1s^2 2p$) excitation probability at $E = 5$ keV displays one small peak at the impact parameter $b = 4$ a.u. and a larger peak at $b = 10$ a.u. However, moving to higher collision energy ($E = 15$ keV), the transition probability not only becomes larger but we now also observe only one almost symmetrical peak centered at the impact parameter $b = 8$ a.u. Also note that the major peak tends to shift to a smaller impact parameter as the incident energy is increased. Fourth, we observe that the probability distributions also vary greatly from one transition to the other for both energies.

We have also carried out additional calculations and confirmed that the Li($1s^2 2p$) and Li($1s^2 3l$) excitation cross sections are insensitive (i.e., differ by an average of less than 3%) whether seven channels (with $m = 0, 1, -1, 2, -2, 3, -3$) or nine channels (with $m = 0, 1, -1, 2, -2, 3, -3, 4, -4$) are used in Eq. (3), and whether the number multipoles are increased from $\lambda_{max} = 4$ to $\lambda_{max} = 5$ in Eq. (5). This degree of sensitivity is expected and consistent with the earlier $p + \mathrm{H}$ collision calculations [17].

Next, we examine the convergence of the transition probabilities with respect to propagation time. Figures 5(a) and 5(b)

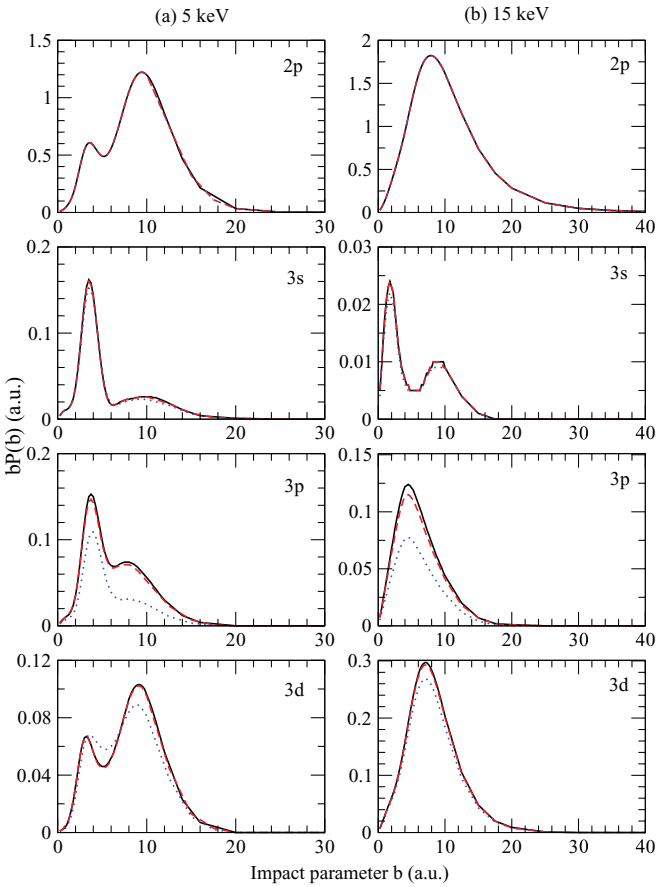

FIG. 4. (Color online) Impact-parameter-weighted excitation probabilities for Li($1s^2 2p$), Li($1s^2 3s$), Li($1s^2 3p$), and Li($1s^2 3d$) transitions as a function of impact parameter b. Black solid line shows TDCC-A, red dashed line shows TDCC-B, and blue dotted line shows TDCC-C.

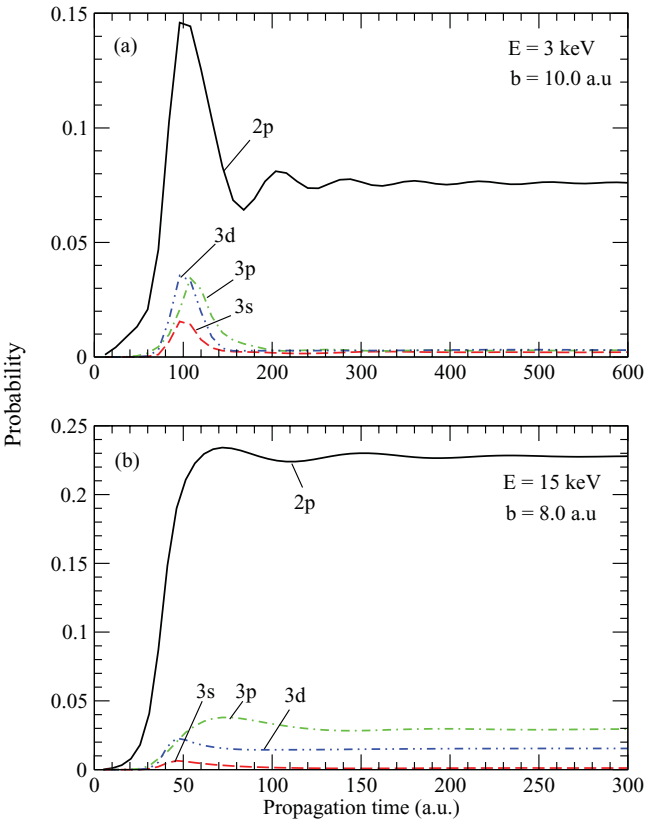

FIG. 5. (Color online) Transition probability for Li($1s^2 2p$) and Li($1s^2 3l$) as a function of propagation time. Black solid line shows $2p$, red dashed line shows $3s$, green dash-dotted line shows $3p$, and blue dash-double-dotted line shows $3d$.

display the Li($1s^2 2p$) and Li($1s^2 3l$) excitation probabilities as a function of propagation time for $E = 3$ keV with $b = 10$ a.u. and $E = 15$ keV with $b = 8$ a.u., respectively. As this figure illustrates, the $n = 3$ manifolds converge relatively fast compared to the case of Li($1s^2 2p$) and a longer time propagation is indeed necessary for Li($1s^2 2p$) to achieve satisfactory convergence, especially for the low collision energies. Note that $b = 8$ and 10 a.u. are chosen for these two energies because the transition probabilities happened to be the largest at these two values.

IV. SUMMARY

A time-dependent close-coupling method, formulated within the framework of a rotational function expansion in two-dimensional cylindrical coordinates, has been extended and used to investigate the excitation processes in proton collisions with atomic lithium. A Hartree-Slater local exchange potential was employed to represent the quasi-one-electron lithium atoms. To first check the present calculation, a comparison was made with the previous Cartesian LTDSE calculations. It is found that the present TDCC-calculated Li($1s^2 2p$) cross sections are in reasonable agreement with the LTDSE results for collision energies of 5, 10, and 15 keV. As a result, further and larger calculations were carried out to determine the Li($1s^2 2s$) $\rightarrow$ Li($1s^2 2p$) as well as Li($1s^2 3l$) excitation cross sections for proton incident energies ranging between 2 and 50 keV. When comparing the two TDCC calculations, it is found that the choice of $\alpha = 0.25$ gave better lithium binding energies and yielded Li($1s^2 2p$) cross sections notably higher than the choice of $\alpha = 0.74$. We attribute the difference between the two TDCC calculations to the difference in the $\Delta E_{2s\text{-}2p}$ energy gap between the two calculations. Further comparisons are made and showed that the TDCC-calculated Li($1s^2 2p$) cross sections as a function of collision energy are generally in suitable agreement with the experimental data as well as atomic-orbital close-coupling calculations. In the case of the $n = 3$ manifold transitions, we also found a somewhat similar behavior. In view of the demonstrated notable effect of the local exchange α parameter on the excitation cross sections, we shall consider in a future study a parameter-free optimized-potential method [21] to better represent a quasi-one-electron atom, which might give more accurate inelastic cross sections.

Results from several sets of lattice calculations based on different box sizes, the number of rotational channels, the propagation time, and the variations of the local exchange potential parameter α are examined and shown to support the convergence and degree of accuracy of the state-selective excitation cross sections presented, especially for the weaker Li($1s^2 3l$) transitions.

In the future, we plan to apply the TDCC method to further investigate the heavy-particle excitation of atoms needed for diagnostics of controlled fusion plasmas. In addition, we will further develop the method to study proton-impact charge transfer with atoms.

ACKNOWLEDGMENTS

This work was supported in part by grants from the US Department of Energy and the US National Science Foundation. Computational production work was carried out at the National Energy Research Scientific Computing Center in Oakland, California and at the National Institute for Computational Sciences in Knoxville, Tennessee.

[1] R. Fischer, E. Wolfrum, J. Schweinzer (the ASDEX Upgrade Team), Plasma Phys. Controlled Fusion **50**, 085009 (2008).
[2] M. Brix, D. Dodt, A. Korotkov, P. Morgan, D. Dunai, R. Fischer, A. Meigs, I. S. Nedzelskiy, J. Schweinzer, J. Vince, S. Zoletnik, and JET-EFDA contributors, Rev. Sci. Instrum. **81**, 10D733 (2010).
[3] F. Aymayr, M. Fehringer, and HP. Winter, J. Phys. B **17**, 4185 (1984).
[4] F. Aymayr, M. Fehringer, and HP. Winter, J. Phys. B **17**, 4201 (1984).
[5] F. Aymayr, G. Lakits, W. Hisinsky, and HP. Winter, J. Phys. B **18**, 2493 (1985).
[6] C. Stary, H. Lüdde, and R. M. Dreizler, J. Phys. B **23**, 263 (1990).
[7] R. Brandenburg, J. Schweinzer, F. Aymayr, and HP. Winter, J. Phys. B **31**, 2585 (1998).
[8] J. W. Turkstra, D. Meyer, R. Hoekstra, R. Morgenstern, and J. J. Schweinzer, Phys. Rev. A **60**, 4627 (1999).
[9] M. S. Pindzola, Phys. Rev. A **60**, 3764 (1999).
[10] L. Nagy and S. Fritzsche, J. Phys. B **33**, L495 (2000).
[11] A. Lühr and A. Saenz, Phys. Rev. A **77**, 052713 (2008).
[12] D. R. Schultz, M. R. Strayer, and J. C. Wells, Phys. Rev. Lett. **82**, 3976 (1999).
[13] D. R. Schultz, C. O. Reinhold, P. S. Krstic, and M. R. Strayer, Phys. Rev. A **65**, 052722 (2002).
[14] M. S. Pindzola, Phys. Rev. A **66**, 032716 (2002).
[15] M. S. Pindzola, T. Minami, and D. R. Schultz, Phys. Rev. A **68**, 013404 (2003).
[16] T. Minami, M. S. Pindzola, T. G. Lee, and D. R. Schultz, J. Phys. B **39**, 2877 (2006).
[17] M. S. Pindzola and D. R. Schultz, Phys. Rev. A **77**, 014701 (2008).
[18] C. F. Fischer, Comput. Phys. Commun. **43**, 355 (1987).
[19] [http://physics.nist.gov/PhysRefData/ASD/levels_form.html].
[20] M. S. Pindzola, F. Robicheaux, N. R. Badnell, and T. W. Gorczyca, Phys. Rev. A **56**, 1994 (1997).
[21] J. D. Talman and W. F. Shadwick, Phys. Rev. A **14**, 36 (1976).